

Bringing Age Back In: Accounting for Population Age Distribution in Forecasting Migration

Nathan G. Welch¹, Hana Ševčíková², and Adrian E. Raftery³

¹Department of Statistics, **University of Washington**,
Box 354322, Seattle, WA 98195-4322, USA
Email: nwelch@uw.edu

²Center for Statistics and the Social Sciences, **University of Washington**,
Box 354322, Seattle, WA 98195-4320, USA
Email: hanas@uw.edu

³Departments of Statistics and Sociology, **University of Washington**,
Box 354322, Seattle, WA 98195-4322, USA
Email: raftery@uw.edu

March 12, 2024

Abstract

The link between age and migration propensity is long established, but existing models of country-level net migration ignore the effect of population age distribution on past and projected migration rates. We propose a method to estimate and forecast international net migration rates for the 200 most populous countries, taking account of changes in population age structure. We use age-standardized estimates of country-level net migration rates and in-migration rates over quinquennial periods from 1990 through 2020 to decompose past net migration rates into in-migration rates and out-migration rates. We then recalculate historic migration rates on a scale that removes the influence of the population age distribution. This is done by scaling past and projected migration rates in terms of a reference population and period. We show that this can be done very simply, using a quantity we call the *migration age structure index* (MASI). We use a Bayesian hierarchical model to generate joint probabilistic forecasts of total and age- and sex- specific net migration rates over five-year periods for all countries from 2020 through 2100. We find that accounting for population age structure in historic and forecast net migration rates leads to narrower prediction intervals by the end of the century for most countries. Also, applying a Rogers & Castro-like migration age schedule to migration outflows reduces uncertainty in population pyramid forecasts. Finally, accounting for population age structure leads to less out-migration among countries with rapidly aging populations that are forecast to contract most rapidly by the end of the century. This leads to less drastic population declines than are forecast without accounting for population age structure.

keywords: *migration, probabilistic, population, projection, forecast*

1 Introduction

Preparations for the next great demographic era are underway around the world (C. J. Kim, 2019; Director of National Intelligence, 2021). Decades of declining and then sub-replacement fertility created a demographic dividend, where the share of the working-age population far outweighed the share of children and older adults no longer participating in the workforce (Bongaarts, 2009). Now the average ages of populations around the world are increasing at the fastest rate in history (Bloom & Zucker, 2023). International migration may blunt the impact of this dynamic, but migration alone will not fully mitigate the realities of the next demographic era (RAND, 2005; Coleman, 2008). Accounting for past and forecast population age structure reveals that migration may be an even less effective mitigation than currently understood (Münz, 2013; Lee, 2011). However, existing forecasting methods fail to account for this eventuality, leaving the role of population age structure in migration dynamics to imprecise qualitative conjecture.

In the period from 2000 through 2015, growth in the total number of migrants in developed countries averaged 3.0% annually, outpacing the 0.6% annual population growth in these nations (Woetzel et al., 2016). More robust forecasts of migration dynamics are critical to the long-term policymaking process as countries compete for the same migrants to mitigate the impacts of sustained sub-replacement birth rates. In the coming decades, the portfolio of migrant supplying countries will have to evolve as birth rates fall, origin populations age, and the share of migration-age people in historic migrant supplying countries falls.

We propose a probabilistic net migration forecasting approach that accounts for the impacts that population age structure had on historic migration rate estimates. We use these to generate new probabilistic population forecasts for all countries. The resulting forecasts quantify how different the global population distribution could be after accounting for past and projected shifts in the population age structure.

The article is organized as follows. Section 2 describes the background to our study. Section 3 summarizes the data and methods used to generate age standardized migration forecasts. It details each step of the population forecasting method. This is followed in Section 4 by an evaluation of the age-standardized migration method compared to forecasts that do not account for the role of population age structure in population forecasting. Then Section 5 summarizes differences between population forecasts with and without accounting for population age structure in the migration component of the forecasts. We conclude in Section 6 with a discussion of the contributions and limitations of our approach.

2 Background

The association between migration and age is long established. Rogers & Castro (1981) identified a consistent pattern in the age profile of out-migrants and proposed a model migration age schedule. Even though modern migration estimation and forecasting methods use migration age schedules to account for the impact of migration on the sending and receiving populations, population age structure is rarely an explicit consideration in estimation or forecasting. This is reasonable over short-term forecast horizons given the relatively slow pace of population age structure changes, but less so over the long term.

Kupiszewski (2002) discussed differences in migration forecasts when the sending population age-structure is ignored. Specifically, it was argued that ignoring the limited

number of migration-age individuals in Poland and ignoring natural population aging contributed to unrealistically large out-migration forecasts from Poland to other European Union (EU) countries before accession to the EU in 2004.

Fertig & Schmidt (2005) argued that neglecting population age in calculating migration rates obscures the underlying population dynamics. They proposed an adjusted net migration rate that is calculated as the number of migrants aged 0-39 divided by the sending country population aged 0-39. This approach reduces distortions created by the population of older people who tend to make up a relatively small proportion of migrants, but effectively sets older age migration to zero and ignores the age structure of the critical 0-39 age group.

Kolk (2019) reviewed age-specific migration and the analogy to age-specific and total fertility rate definitions. It was argued that population-level measures should be adopted for both subnational and international migration estimation. The authors outlined key challenges to extending such methods to an international context, specifically properly specifying the population at risk of in-migration and differences in the definition of an international migrant from country to country.

Fully probabilistic population forecasting is an active area of demographic research (e.g. Hyndman & Booth, 2008; Raftery et al., 2012, 2014; Wiśniowski et al., 2015; Yu et al., 2023). Azose et al. (2016) developed a probabilistic net migration model and used it to produce probabilistic population forecasts for all countries through 2100. Welch & Raftery (2022) proposed a fully probabilistic population forecasting method that uses a probabilistic model of bilateral migration flows for all countries through 2045. However, none of these population forecasting methods systematically account for population age structure changes in both the historic data used to fit these models and in forecasting.

Raftery & Ševčíková (2023) proposed a method for accounting for population age structure in probabilistic migration and population forecasts, and applied it to very long term population forecasts, to 2300, motivated by the problem of estimating the social cost of carbon. Like us, they used net migration data, which has advantages of data availability and analytical simplicity over methods based on more complete migration data, such as between-country flows or in- and out-migration flows for countries. However, a problem with this is that it does not take account of the different age distributions of in- and out-migrants (Rogers, 1990). They avoided this problem by assuming that when a country experienced net in-migration in a period, it was all in-migration and there was no out-migration, and conversely for out-migration. Here we develop a new method that avoids this unrealistic assumption while still using net migration data.

3 Data & Methods

Data

Recent methodological innovations make it possible to estimate globally consistent country-level total migration inflows and outflows from Census counts of the number of people by country of birth in all countries (Abel, 2013; Azose & Raftery, 2019). Abel & Cohen (2019) found that the pseudo-Bayes method of Azose & Raftery (2019) to estimate bilateral migration flows led to the most accurate migration estimates among several extant methods. Unfortunately, pseudo-Bayes migrant flow estimates over five-year periods are available for only six five-year periods starting in 1990 and ending in 2020 (Abel & Cohen, 2019). Estimating and forecasting bilateral migration flows has a number of advantages

(Welch & Raftery, 2022), but population age structure changes too slowly to solely rely on these estimates for long-term migration forecasting.

The United Nation’s World Population Prospects (WPP) publishes globally consistent net migration estimates back to the 1950-1955 period (United Nations, 2022). The net migration rate is defined as the difference between migration inflows and outflows divided by population size. As such, the population age structure at the given time is not accounted for.

The pseudo-Bayes flow estimates and net migration rate estimates have independent value. The pseudo-Bayes flow estimates contain more detailed information in the form of bilateral flows, but the length of such time series is limited (Abel & Cohen, 2019). On the other hand, the availability of net migration rate estimates going back to 1950 provides a measure of migration over many more historic periods (United Nations, 2022). We use strengths of both data sets to develop a new combined data series. Migration flow estimates are calculated with respect to specific revisions of the WPP. The most recent flow estimates were estimated using WPP 2019 (Abel & Cohen, 2019). We use WPP 2019 (United Nations, 2019) and the associated flow estimates for all analyses.

We fit a model, described in Section 3, to the 1990-2020 period from which both in-migration and net migration rates can be estimated for all countries with populations of 100,000 or more. This model is then used to approximate the contribution that in-migration made to the net migration rate prior to 1990. Our model-based approach is an efficient solution that allows for the estimation of globally consistent age-standardized in-migration and out-migration rates for five-year periods starting in 1950 and running through 2020. The successful decomposition of net migration rates into in-migration and out-migration rates is critical to calculating migration rates adjusted for the population age structure that gave rise to those rates.

Age Standardization of Net Migration Rates

For reasons of data availability across all countries, and analytic simplicity, the UN uses all-age net migration as part of the basis for its population projections for all countries (United Nations, 2019). They project this forwards deterministically, combining it with probabilistic projections of fertility and mortality, to obtain probabilistic population projections conditional on the projected levels of future migration. As an alternative, Azose & Raftery (2015) proposed a probabilistic approach to forecasting future net migration rates (i.e. net migration divided by population). Neither the UN’s deterministic approach nor the probabilistic approach of Azose & Raftery (2015) takes account of historic or future changes in population age structure.

We propose to modify the approach of Azose & Raftery (2015) to account for population age structure. We do this by creating an age-standardized version of the net migration rate. This is tricky, because historic net migration data are not disaggregated by age. Also, net migration is equal to in-migration minus out-migration, and the age profiles of in- and out-migration can differ. As pointed out by Rogers (1990), this makes it hard to standardize net migration rates directly, and indeed this was one of the arguments of Rogers (1990) for not using net migration at all. Here we propose a method for doing so which hopefully reduces these concerns.

We start by developing a method for decomposing historic net migration into in- and out-migration. This uses a subset of the data for which estimates of both in- and out-migration are available (i.e. 1990-2020), and uses this to estimate in- and out-migration for

the entire data period (i.e. 1950-2020). We then develop a method for age-standardizing out-migration. This turns out to be very simple, relying on a quantity we call the *migration age structure index* (MASI). We extend this to in-migration, and hence to net migration. Finally we apply the probabilistic forecasting method of Azose & Raftery (2015) to the age-standardized net migration rates, and input the resulting forecasts to the overall probabilistic population projection method. The notation used in describing our method is shown in Table 1.

Table 1: Notation for migration age-standardized migration method

$O_{i,t}$	Integer-valued outflow from origin i in period starting with year t
$O_{i,t,a}$	Integer-valued outflow from origin i in period starting with year t of age group a -($a + 4$)
$I_{i,t}$	Integer-valued inflow to destination i in period starting with year t
$N_{i,t}$	Integer-valued net migrant flow in country i in period starting with year t
$P_{i,t,a,s}$	Integer-valued population of origin i at the start of period t for age group a -($a + 4$) and sex $s \in \{\text{male, female}\}$
$P_{i,t,+,+}$	Integer-valued population of origin i at the start of period t
$\tilde{P}_{i,t,+,+}$	Integer-valued population of origin i at risk of migration over period t to $t + 5$, defined as $P_{i,t+5,+,+} - N_{i,t}$
$\text{OMR}_{i,t}$	$= O_{i,t}/\tilde{P}_{i,t,+,+}$. Out-migration rate for country i in the period starting in year t
$\text{OMR}_{i,t,a}$	$= O_{i,t,a}/\tilde{P}_{i,t,a,+}$. Out-migration rate for country i , period starting in year t and age group a
$G_{i,t}$	$= \sum_a \text{OMR}_{i,t,a}$. Gross Migraproduction Rate (GMR) for country i and period starting in year t
$\text{IMR}_{i,t}$	$= I_{i,t}/\tilde{P}_{i,t,+,+}$. In-migration rate for period starting in year t & country i
$\text{NMR}_{i,t}$	$= \text{IMR}_{i,t} - \text{OMR}_{i,t}$. Net migration rate for country i & period t
$\pi_{i,t,a}$	$= \tilde{P}_{i,t,a,+}/\sum_a \tilde{P}_{i,t,a,+}$. Share of population from age group a in period t
$\pi_{i,t,a}^*$	Reference population age distribution for country i in period t
R_a	Reference migration age schedule normalized so that $\sum_a R_a = 1$
$C_{i,t}$	$= \sum_a R_a \pi_{i,t,a}$. The migration age structure index (MASI), a scalar accounting for the population and migrant age structure in the migration rate at time t for country i
\check{C}_t	$= \sum_{i,a} R_a \pi_{i,t,a}$. MASI for the world at time t
$\text{OMR}_{i,t}^*$	$= \text{OMR}_{i,t} \times C_{i,\text{baseline}}/C_{i,t}$. Age-standardized out-migration rate
$\text{IMR}_{i,t}^*$	$= \text{IMR}_{i,t} \times \check{C}_{\text{baseline}}/\check{C}_t$. Age-standardized in-migration rate
$\text{NMR}_{i,t}^*$	$= \text{IMR}_{i,t}^* - \text{OMR}_{i,t}^*$. Age-standardized net migration rate

Decomposing Historic Net Migration into In- and Out-migration

Net migration age-standardization takes place on the inflow and outflow components of the net migration rate. Pseudo-Bayes estimates (Azose & Raftery, 2019; Abel & Cohen, 2019) of migration flows are available over five-year periods starting in 1990 and ending in 2020 (6 periods). Net migration rate estimates are available for five-year periods back to 1950 (United Nations, 2019). We use a mixed-effects model to relate the 1990-2020 in-migration rate, $\text{IMR}_{i,t}$, to the net migration rate, $\text{NMR}_{i,t}$, for each country i over these six five-year periods, t , from 1990 through 2020. Our mixed-effects model is defined as

follows:

$$\begin{aligned}
\text{IMR}_{i,t} &= \beta_{0,i} + \beta_1 \max(\text{NMR}_{i,t}, 0) + \varepsilon_{i,t}, \\
\beta_{0,i} &\sim \text{Normal}(\beta_0, \sigma_{\text{between}}^2), \\
\varepsilon_{i,t} &\sim \text{Normal}(0, \sigma_{\text{within}}^2).
\end{aligned} \tag{1}$$

This model uses a random intercept term to account for the average country-specific in-migration rate associated with the net migration rate for each period from 1990-2020. Country intercepts, $\beta_{0,i}$, are concentrated around a global mean intercept, β_0 . The difference in a country's random intercept from the global mean, β_0 , is determined by the average difference from the global mean for that country in all periods. Outflow rates are implicitly defined by this model. Table 1 defines each term in the model.

The random intercept model was fit using the linear mixed-effects model implementation in the *lme4* R package implementation (Bates et al., 2015). Starting with $\text{NMR}_{i,t}$, the estimated in-migration rate is $\text{IMR}_{i,t} = \beta_{0,i} + \beta_1 \max(\text{NMR}_{i,t}, 0)$. The net migration rate and estimated in-migration rate are then used to calculate the out-migration rate, $\text{OMR}_{i,t} = \text{IMR}_{i,t} - \text{NMR}_{i,t}$.

Figure 1 summarizes the 1990-2020 data, model fit, and association between estimated and actual country-level migration flow rates. Points in Figure 1(a) show the observed $\max(\text{NMR}_{i,t}, 0)$ on the horizontal axis and $\text{IMR}_{i,t}$ on the vertical axis. The discontinuity at $\text{NMR}_{i,t} = 0$ reflects the fact that the in-migration rate must be non-negative. In the $\text{NMR}_{i,t} \leq 0$ portion of the domain, the country-specific intercept, $\beta_{0,i}$, of model 1 establishes the minimum average magnitude of in-migration corresponding to a negative net migration rate for that country. When $\text{NMR}_{i,t} > 0$, the model in-migration rate increases from this minimum average inflow at a rate of β_1 per unit increase in $\text{NMR}_{i,t}$. The mean model in-migration rate is shown by the blue line in Figure 1(a).

Many observations in Figure 1(a) are highly concentrated around some values. The LOESS curve helps clarify the location of points that fall too close to each other to be seen separately. In the $\text{NMR}_{i,t} < 0$ portion of the domain, the similarity between the LOESS line and the $\beta_{0,i}$ values shows that the mean intercept term provides an accurate summary of the observed in-migration and net migration rates. Near $\text{NMR}_{i,t} = 0$, however, the disagreement between the model mean and LOESS line shows that many $\text{IMR}_{i,t}$ observations near $\text{NMR}_{i,t} = 0$ could be overstated with the model mean alone. The LOESS line departs from the mean model most for large positive values of $\text{NMR}_{i,t}$. This is primarily due to the influence of a few large positive $\text{NMR}_{i,t}$ observations for a small number of countries.

Finally, Figure 1(a) shows two examples of country-specific average association between $\text{IMR}_{i,t}$ and $\text{NMR}_{i,t}$. The top line shows the model fit for Qatar (maroon), which experienced some of the highest migration rates in the world since 1990. The bottom line shows the model fit for China, a country with stable net out-migration over the same period. The differences between these two examples highlight the need for a model flexible enough to account for such wide variation between countries.

Figure 1(b) shows the fitted and observed $\text{IMR}_{i,t}$ for all countries from 1990-2020. The high level of agreement between fitted and observed in-migration rates with an $R^2 = 0.98$ is notable considering the simplicity of model (1). The agreement between fitted and observed out-migration rates in Figure 1(c) is lower with $R^2 = 0.91$, but is still strong. Taken together, Figures 1(b)-(c) show that our model-based decomposition of the net migration rate is reasonable for the periods where net migration, in-migration, and out-migration rates are all available.

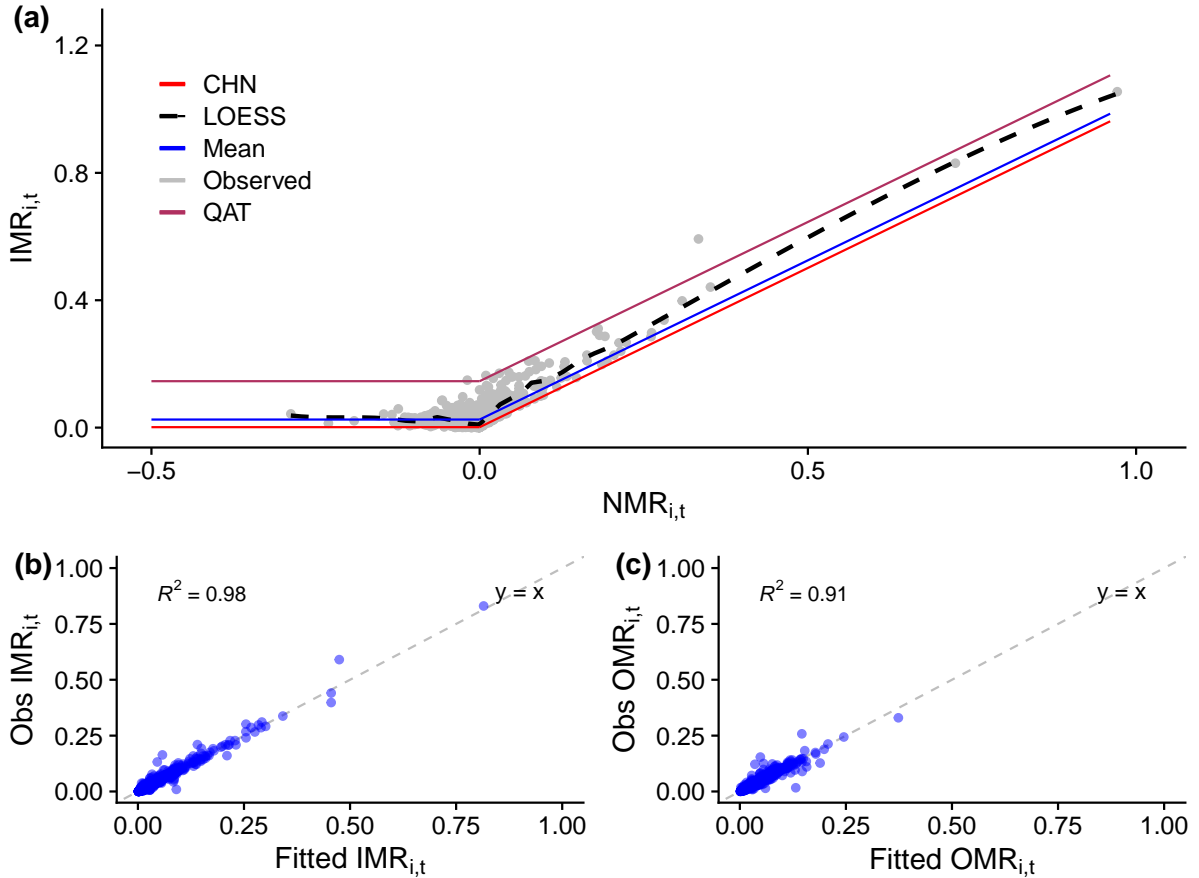


Figure 1: (a) Observed in-migration rates versus net migration rates for all countries (points) with mean model (blue), LOESS line (black dashed), and country-specific models for China (CHN, red) and Qatar (QAT, maroon); (b) Observed in-migration rates versus fitted in-migration rates compared to $y = x$ (dashed line); (c) Observed out-migration rates versus fitted out-migration rates compared to $y = x$ (dashed line) for five-year-periods from 1990-2020.

Figure 2 shows the observed net migration rate for five-year periods starting in 1950 and running through 2020 on the original scales. The inflow and outflow rates from 1990 through 2020 used for the estimation of our model are shown in the second and third columns along with the mixed-effects model decomposition. Our model-based estimates of inflow and outflow rates applied to years prior to 1990 are also shown in the plots. Model-based estimates relating net migration rates to in-migration and out-migration rates are similar to the observed rates for 1990-2020. Estimated inflow and outflow rates prior to the 1990-1995 period appear plausible for the periods where pseudo-Bayes estimates are available.

While the model-based decomposition is not perfect, Figure 2 shows that the mixed-effects net rate decomposition approach leads to plausible estimates of in-migration and out-migration rates. The correlation between the observed and predicted rates was over 0.97. Broad agreement between observed inflow and outflow rates for 1990-2020 periods suggests that net migration rates prior to 1990 can be similarly decomposed into inflow and outflow rates.

Raymer et al. (2023) proposed an alternative approach to decomposing net migration

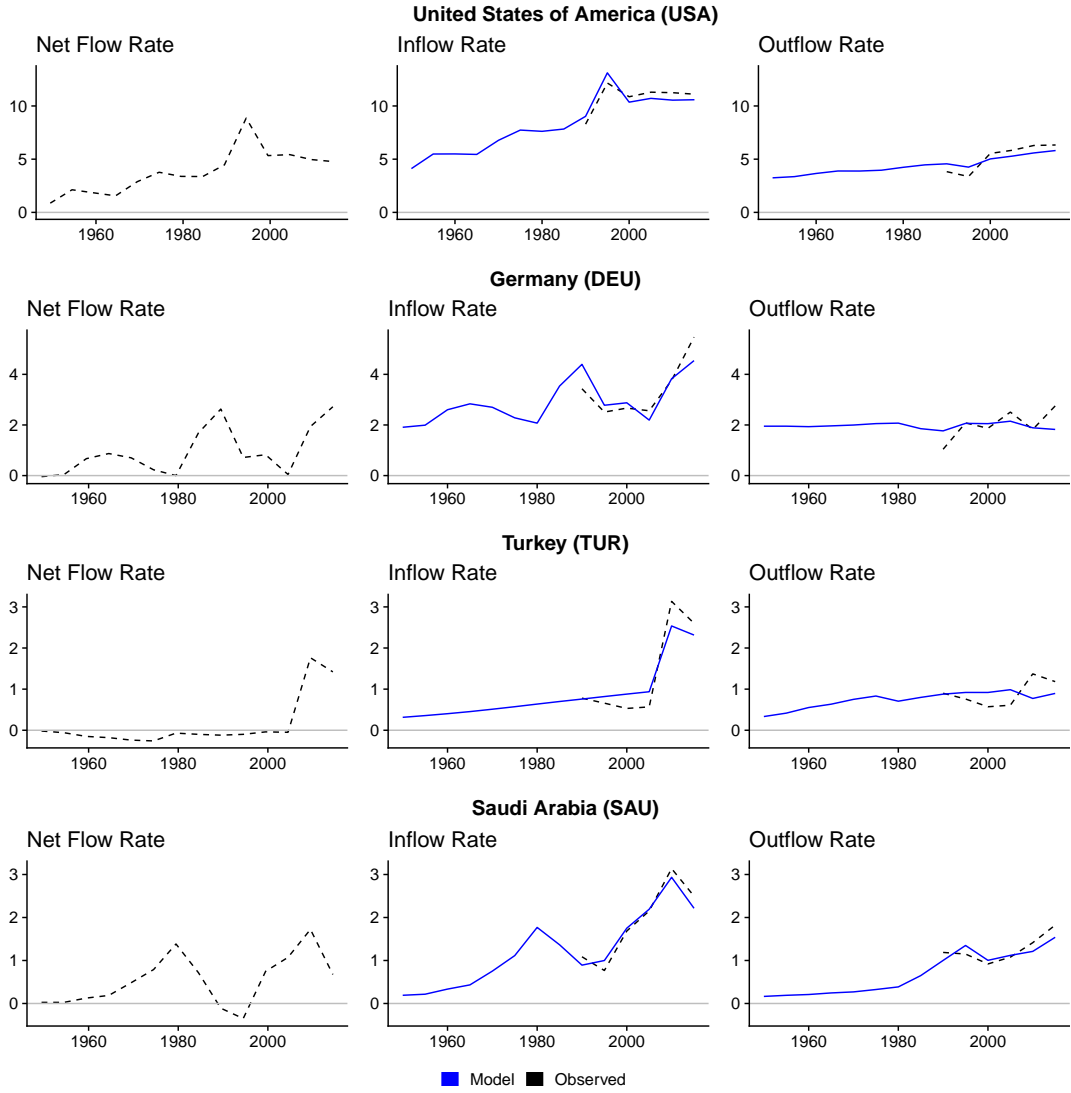


Figure 2: Observed net migration (left column), decomposed into in-migration (middle column), and out-migration rates (right column), on the scale of annual migrants per thousand people, compared to mixed-effects model estimates for the United States, Germany, Turkey, and Saudi Arabia. Solid blue lines show the model-based estimates. Dashed black lines show the observed migration rates used for the estimation.

into in-migration and out-migration. This method uses a fixed constant to approximate the magnitude of net migration attributed to total inflows and outflows in proportion to a country's population. This method could also be used to decompose the net flow into total inflow and outflow in place of model (1) for a subset of countries or all countries if desired. However, we found the proportion of the in-migration to net migration rates using model (1) too variable to justify using a single constant for all countries. The model (1) offers a systematic approach to specifying a quantity similar to the fixed constant used in Raymer et al. (2023), but one that is country-specific, which our analyses suggest is needed.

Age Standardization of Out- and In-migration Rates

The net migration rate, $\text{NMR}_{i,t}$, for country i over period t to $t + 5$ is defined as the difference between the in-migration rate, $\text{IMR}_{i,t}$, and out-migration rate, $\text{OMR}_{i,t}$:

$$\text{NMR}_{i,t} = \text{IMR}_{i,t} - \text{OMR}_{i,t} = \frac{N_{i,t}}{\tilde{P}_{i,t,+,+}} = \frac{I_{i,t} - O_{i,t}}{\tilde{P}_{i,t,+,+}}. \quad (2)$$

Here, $I_{i,t}$ denotes the total inflow count, $O_{i,t}$ the total outflow count, and $N_{i,t} = I_{i,t} - O_{i,t}$ the total net flow count over the period starting in year t . We define the denominator of the net migration rate, $\tilde{P}_{i,t,+,+} = P_{i,t+5,+,+} - N_{i,t}$, as the population of country i at the end of the period starting in year t before factoring in the change due to net migration. This denominator specifies the population at risk of migration over the period.

Historic net migration rate estimates are not disaggregated by age, but we aim to standardize migration rates to remove the effects of population age structure differences among countries in the same period and within countries across periods. The age pattern of age-specific migration rates is known to be relatively consistent over time and country of origin (Rogers & Castro, 1981), but the rate defined in equation (2) obscures the influence of the sending and receiving country population age structures, as discussed by Rogers (1990). A population age-standardized net migration rate should account for the age structure of the sending populations in both components of the net rate as the migrant age distribution and totals are primarily linked to the origin population age structure.

Let $\pi_{i,t,a}$ denote the population in age group a as a proportion of the total population in country i at time t , namely

$$\pi_{i,t,a} = \frac{\tilde{P}_{i,t,a}}{\sum_a \tilde{P}_{i,t,a}}. \quad (3)$$

Since the origin population of inflows to country i consists of every country other than i in period starting in year t , we approximate the proportion of the global population in age-group a by

$$\tilde{\pi}_{t,a} \approx \frac{\tilde{P}_{+,t,a,+}}{\tilde{P}_{+,t,+,+}} \quad \text{where} \quad \tilde{P}_{+,t,a,+} = \sum_{i,s} \tilde{P}_{i,t,a,s} \quad \text{and} \quad \tilde{P}_{+,t,+,+} = \sum_{i,s,a} \tilde{P}_{i,t,a,s}. \quad (4)$$

The out-migration rate for country i , period t and age group a is $\text{OMR}_{i,t,a}$, and $G_{i,t} = \sum_a \text{OMR}_{i,t,a}$ is the *Gross Migraproduction Rate* (GMR) for country i and period t , as defined by Rogers & Castro (1981). This is a measure of overall migration that is not affected by population age distribution, rather as the Total Fertility Rate (TFR) is a measure of overall fertility that is independent of the age distribution of women.

The values of $\text{OMR}_{i,t,a}/G_{i,t}$, which give the age pattern of age-specific out-migration rates, tend to be stable over time and place, reflecting a tendency for international migration to be largely concentrated among people aged 15–35 and their dependent children, peaking in the twenties, as pointed out by Rogers & Castro (1981). They also proposed a parametric model for this pattern, the famous Rogers-Castro curve. As an approximation, we thus consider the situation where this ratio is constant over time and space, so that $\text{OMR}_{i,t,a}/G_{i,t} = R_a$ for all i, t , where $\sum_a R_a = 1$. Under this assumption, the quantity R_a is the same for all countries and time periods, and could be modeled by a Rogers-Castro curve, or estimated empirically.

We then have an exact result for the out-migration rate for a reference population with a given age distribution:

Theorem 1. Consider a population that has the same age-specific out-migration rates as country i in period t , but a different population age distribution given by $\pi_{i,t,a}^*$. Then this population has out-migration rate

$$OMR_{i,t}^* = OMR_{i,t} \frac{\sum_a \pi_{i,t,a}^* OMR_{i,t,a}}{\sum_a \pi_{i,t,a} OMR_{i,t,a}}. \quad (5)$$

If both populations have the same age-specific pattern of migration rates, R_a , then

$$OMR_{i,t}^* = OMR_{i,t} \frac{C_{i,t}^*}{C_{i,t}}, \quad (6)$$

where $C_{i,t} = \sum_a \pi_{i,t,a} R_a$ is the migration age structure index (MASI).

The proof of this theorem can be found in the Appendix.

This indicates that one can age-standardize the out-migration rate to a given reference population using equation (6). This is a remarkably simple method, since it involves only a simple multiplication by the MASI, $C_{i,t}$. The MASI involves only the population age distribution and the invariant migration age-pattern R_a , but not the age-specific migration rates themselves, which cancel.

We can age-standardize in-migration by viewing it as out-migration to country i from the rest of the world. We approximate the age distribution of the rest of the world by the age distribution of the world as a whole. This yields an age-standardized in-migration rate, $IMR_{i,t}^*$. Finally, we obtain the age-standardized net migration rate as $NMR_{i,t}^* = IMR_{i,t}^* - OMR_{i,t}^*$.

Typically the reference population age distribution will be the distribution in a particular year. In this article, we standardize to the age pattern of 2020. To calculate the age-standardized in-migration and out-migration rate of period t in terms of the 2020 population age structure, remove the population age structure effects in period t and scale the migration rate in terms of the 2020 reference population:

$$\begin{aligned} IMR_{i,t}^* &= IMR_{i,t} \frac{\check{C}_{2020}}{\check{C}_t} \\ OMR_{i,t}^* &= OMR_{i,t} \frac{C_{i,2020}}{C_{i,t}} \end{aligned} \quad (7)$$

where \check{C}_t denotes the MASI for the world at time t .

This implies that the age-standardized net migration rate is given by $NMR_{i,t}^* = IMR_{i,t}^* - OMR_{i,t}^*$. This measure of migration puts historic and forecast rates of migration into the context of the 2020 population age structure, removing variation in migration rates attributable to population age structure differences from period to period. This specification also shows how to convert between the age-standardized rates and the historic or future rates in terms of the reference population.

After estimating historic inflow and outflow rates calculated from model (1), age-standardized inflow, outflow, and net flow rates can be calculated for forecasting.

Net Migration Rate Model

We use the resulting rates to develop a probabilistic model for age-adjusted net migration rates. Using the above estimates of inflows and outflows, we compute the age-standardized net migration rates, $NMR_{i,t}^*$, for all countries i and for t from 1950 through

2020, using the 2020 population age structures as the baseline population, as shown in Section 3. We then fit the Bayesian hierarchical model of Azose & Raftery (2015). Hyperparameter values for this model required no adjustment since the default specifications were broadly defined and our specification of the net rate is on the same scale as that of Azose & Raftery (2015). This is done using a Markov chain Monte Carlo (MCMC) algorithm. This yields a sample of model parameters.

Forecasting

The goal here is to forecast migration and population probabilistically by generating jointly a set of future migration and population trajectories. We use the same approach to forecasting fertility and mortality as the UN projections for the UN’s 2019 *World Population Prospects* (WPP) (United Nations, 2019). Our approach to forecasting migration builds on the methods of Azose & Raftery (2015) and Azose et al. (2016), but modifies them to adjust for differences in population age distribution over time and between countries.

For each future trajectory $j \in \{1, \dots, J\}$, we independently project the population for each country i by five-year age group a through $a + 5$ and sex s for year $t + 5$ without migration. The resulting projection, $\tilde{P}_{i,t+5,a,s}^{(j)}$, denotes a realization of the total population that would be observed in year $t + 5$ had no one in the population migrated in or out of each country. This approximates the population at risk of migrating for the period t to $t + 5$, by age and sex. We then independently generate an age-standardized net migration rate for the period t to $t + 5$, $\text{NMR}_{i,t}^{*(j)}$, using the parameter sample from the Bayesian hierarchical model of Azose & Raftery (2015) estimated in the previous subsection. The sampled age-standardized net migration rate is then decomposed into the age-standardized in-migration rate, $\text{IMR}_{i,t}^{*(j)}$, and age-standardized out-migration rate, $\text{OMR}_{i,t}^{*(j)}$, using the mixed-effects model (1) that has been fit to age-standardized historical rates (i.e., IMR^* and OMR^*). The resulting age-standardized coefficients are denoted by β_0^* and β_1^* .

The mean age-standardized in-migration rate for trajectory j and country i is calculated as

$$\text{IMR}_{i,t}^{*(j)} = \beta_{0,i}^* + \beta_1^* \max\left(\text{NMR}_{i,t}^{*(j)}, 0\right). \quad (8)$$

The corresponding out-migration rate for the period starting in year t is then given by

$$\text{OMR}_{i,t}^{*(j)} = \text{IMR}_{i,t}^{*(j)} - \text{NMR}_{i,t}^{*(j)}. \quad (9)$$

Age-standardized inflow and outflow rates then need to be converted back to period-specific rates to calculate inflow and outflow counts corresponding to the projected population age structure:

$$\begin{aligned} \text{IMR}_{i,t}^{(j)} &= \text{IMR}_{i,t}^{*(j)} \times \check{C}_t^{(j)} / \check{C}_{2020}, \\ \text{OMR}_{i,t}^{(j)} &= \text{OMR}_{i,t}^{*(j)} \times C_{i,t}^{(j)} / C_{i,2020}. \end{aligned} \quad (10)$$

In-migration rates then are converted to inflow counts by age and sex, $I_{i,t,a,s}^{(j)}$, by multiplying the inflow rate by the total country population for trajectory j at time t and then applying a Rogers & Castro-like migration age schedule. These counts are further disaggregated by sex in proportion to the males and females in the population. Out-migration counts by age and sex, $O_{i,t,a,s}^{(j)}$, are similarly calculated.

While a Rogers & Castro-like age schedule is appropriate for out-migration in most countries, the migration schedules in Gulf Cooperation Council (GCC) member states (Bahrain, Kuwait, Oman, Qatar, Saudi Arabia, United Arab Emirates) call for a different approach. In recent decades, GCC country migration has been dominated by large inflows of primarily male migrant workers. This workforce supplies the labor required to power some of the globe’s largest construction and infrastructure projects. These temporary workers typically enter GCC countries on visas valid for two years or less. The path from temporary worker to long-term resident or citizen is nearly nonexistent in GCC countries. As a result, the population age structure of GCC countries should be influenced by changes in the volume of migrant workers, but the age distribution of the population should remain relatively constant as worker visas expire, those workers leave the country, and new workers arrive to replace them or add to their ranks. To maintain the population age structure of the population due to temporary workers, we take a different approach to the migration age schedule.

Instead of applying the standardized model migration age schedule in GCC countries, we used a different schedule to maintain the foreign-worker-dominated age structure. This modification ensures that the population age distribution in GCC countries remain consistent with the distribution of migrant worker stocks replaced by departing foreign workers. The out-migration schedule was modified so that outflows are dominated by older working age migrants, instead of the Rogers & Castro-like schedule used for all other countries. After accounting for the age distribution of the population due to immigration, the outflow migration age schedule was determined by the difference between the population age distribution and the normalized Roger & Castro-like migration age schedule. This formulation effectively re-weights the outflow schedule so that outflows are composed of older workers aging out of prime working age groups (i.e., 15–65). Outflow rates in GCC countries have been much smaller than inflow rates over recent decades, but the population age distribution has changed little over this time. Hence, these inflow and outflow migration schedule modifications ensure that the migrant worker population remains in the prime working age range rather than having large groups of migrant workers aging in place with the resident population. We found that these adjustments led to much more plausible forecasts of GCC migration and population dynamics through 2100 compared to the approach used for the rest of the world.

It was necessary to rebalance global inflows and outflows each period to maintain global net-zero migration. Azose & Raftery (2015) and Azose et al. (2016) proposed methods for doing so, but their methods are not directly applicable to a forecasting method that produces inflow and outflow counts for each country. Adjusting net migration counts without specifying the proportion allocated to inflows or outflows leads to inconsistencies in the projected inflow and outflow totals compared to the net flow totals. We adjusted inflow and outflow totals by the global net overflow/underflow by adjusting inflow and outflow totals at the country-level in proportion to the country population as a share of the globe.

The global rebalancing procedure is as follows. Let $\tilde{I}_{i,t,a,s}^{(j)}$ denote the j^{th} inflow count trajectory for country i for period starting in year t for age group a to $a+5$ and sex s . Similarly, let $\tilde{N}_{i,t,a,s}^{(j)}$ denote the corresponding net migration count before global rebalancing.

Then the adjusted inflow and outflow counts were calculated as

$$\begin{aligned} I_{i,t,a,s}^{(j)} &= \tilde{I}_{i,t,a,s}^{(j)} - w \left(\sum_{k \in K} \tilde{N}_{k,t,a,s}^{(j)} \right) \frac{\tilde{P}_{i,t,a,s}^{(j)}}{\sum_{k \in K} \tilde{P}_{k,t,a,s}^{(j)}}, \\ O_{i,t,a,s}^{(j)} &= \tilde{O}_{i,t,a,s}^{(j)} + (1 - w) \left(\sum_{k \in K} \tilde{N}_{k,t,a,s}^{(j)} \right) \frac{\tilde{P}_{i,t,a,s}^{(j)}}{\sum_{k \in K} \tilde{P}_{k,t,a,s}^{(j)}}, \end{aligned} \quad (11)$$

with $w = 0.5$, splitting the global net overflow/under-flow equally among inflows and outflows. The index K defines two groups of countries used for normalization. Rebalancing was done among GCC countries (Bahrain, Kuwait, Oman, Qatar, Saudi Arabia, United Arab Emirates) and the labor supplying origin countries (Bangladesh, India, Indonesia, Philippines, Pakistan) in one group. The second group was composed of all other countries outside the GCC labor corridor. After this adjustment, the global net migration for each age group and sex equals zero and the net flow of migrants for trajectory j in country i at time t by age and sex becomes $N_{i,t,a,s}^{(j)} = I_{i,t,a,s}^{(j)} - O_{i,t,a,s}^{(j)}$. As in Azose & Raftery (2015), these adjustments led to relatively small changes to forecasts.

We then recalculated the balanced age-standardized net migration rate, $\text{NMR}_{i,t}^{*(j)}$, as

$$\text{NMR}_{i,t}^{*(j)} = \left(\frac{I_{i,t,+,+}^{(j)}}{\tilde{P}_{i,t+5,+,+}^{(j)}} \right) \times \check{C}_{2020} / \check{C}_t^{(j)} - \left(\frac{O_{i,t,+,+}^{(j)}}{\tilde{P}_{i,t+5,+,+}^{(j)}} \right) \times C_{i,2020} / C_{i,t}^{(j)}, \quad (12)$$

which will be the rate jump-off for sampling in the next time period. Finally, we account for net migration in the population projection generated at the start of the forecasting routine,

$$P_{i,t+5,a,s}^{(j)} = \tilde{P}_{i,t+5,a,s}^{(j)} + N_{i,t,a,s}^{(j)}, \quad (13)$$

before moving to the next forecast period.

4 Validation

Age-standardized forecast efficacy was evaluated in terms of out-of-sample performance. Figure 3 shows the observed and four-period migration and population forecasts for four countries starting in the 2000-2005 period through the 2015-2020 period. Columns show the United States, El Salvador, South Africa, and Saudi Arabia forecasts using 1995-2000 migration rate persistence (effectively the current UN method) for every period, the age-agnostic method of Azose et al. (2016), and the age-standardized method described above. Rows show the migration age structure index (MASI) ratio, i.e. the ratio of the MASI for the period to the MASI for the baseline year 2000, the net migration rate, and population for each country. Prediction intervals for both the age-agnostic and age-standardized method included the observed population and net migration rates in all cases. Population and migration forecasts using the age-standardized approach were as good or better than the age-agnostic forecasts by the end of the period for all cases except in El Salvador in terms of agreement with the observed quantities. Persistence of 1995-2000 migration rates performed especially poorly for El Salvador and Saudi Arabia.

Age-standardized and age-agnostic forecasts largely agree with one another since population age structure differences make little impact over such a short period of time. Note that the proportion of the migration age population increased relative to the baseline population in El Salvador. The 0–15 year olds were the largest proportion of the population

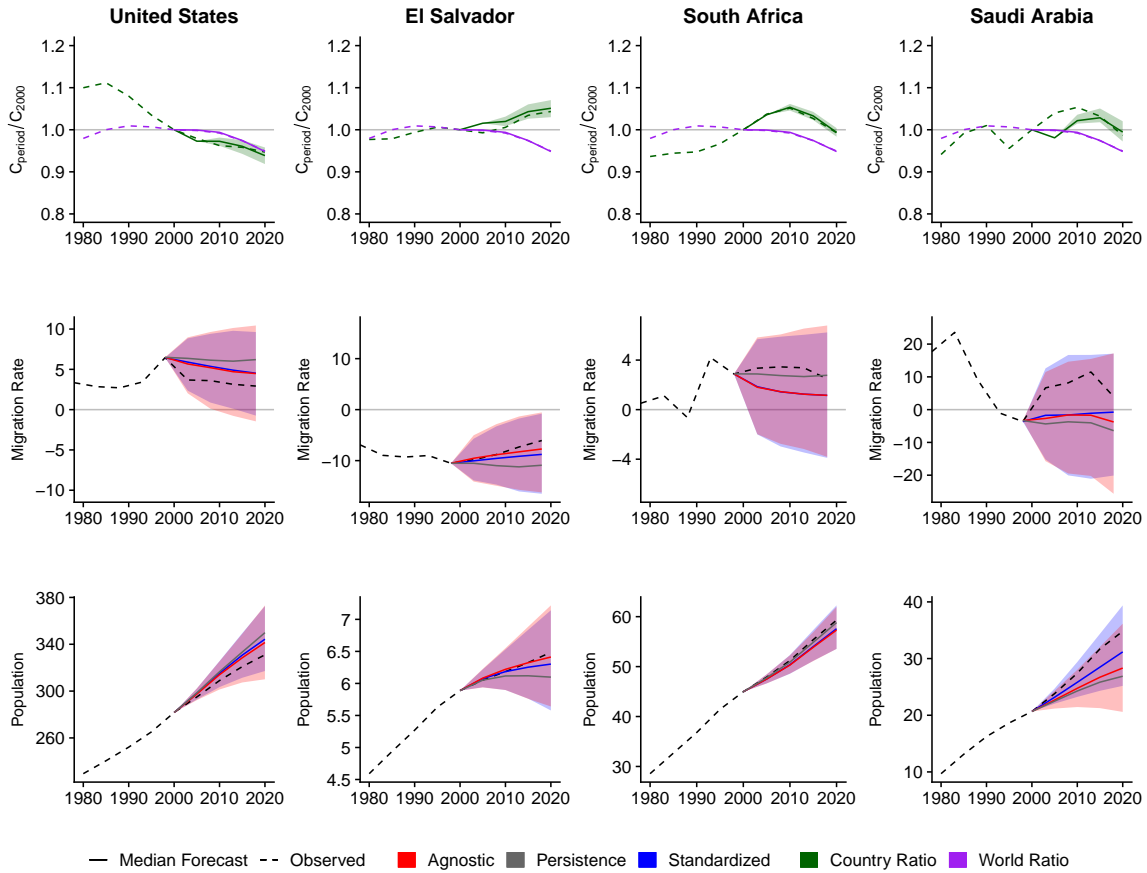


Figure 3: Migration age structure index (MASI) ratio for each country (■) and the globe (■) with base-year 2000, out-of-sample validation forecast of population (millions of people), and age-standardized and age-agnostic net migration rate (net annual migrants per thousand), for four countries. Forecasts use probabilistic age-standardized net migration (■), probabilistic age-agnostic net migration (■), observed fertility, and observed mortality. Dashed lines in each plot indicate the observed values. Solid lines indicate the median forecast. Shaded regions show the 80% prediction interval. Migration models were fit to 1950-2000 data. Forecasts are for the 2000-2005, 2005-2010, 2010-2015 and 2015-2020 periods.

in 2000; however, the proportion of the population aged 0–15 fell during the validation period and the large 0–15 population cohort aged into the prime migration age cohorts by the end of the 2015-2020 period. As a result, El Salvador’s age structure ratio increased from the 2000 baseline period. The age structure ratio forecast outpaced the observed age structure ratio for the first two periods (2000-2010), but the prediction interval contained the observed age structure ratio for the last two periods (2010-2020).

Global age ratio forecasts were well aligned with the true global age structure. Country-level population age ratio forecasts showed mixed results, however. Prediction intervals for the MASI ratio captured all or most of the observed values for the United States and South Africa. The forecast MASI ratio for Saudi Arabia was lower than the true value for the first two periods, but included the observed value by the end of the forecast period. The forecast MASI ratio for El Salvador was consistently higher than the observed value from 2000 to 2010. These departures from the forecast are explained by the higher net migration observations compared to the forecasts for those countries.

Global and country-level MASI ratio values equal one for the baseline population structure (2000 in this case) by definition. When the global MASI is higher than the country-level MASI, then we expect higher in-migration using the age-standardized method compared to the age-agnostic method. Conversely, when the country-level MASI ratio is below 1, we expect lower net out-migration compared to the baseline period using the age-standardized method and a model that does not account for population age structure. The MASI for the United States was below the global MASI and the baseline MASI value for the whole forecast period. The United States' MASI ratio also indicated an aging population compared to the baseline population age structure. Both of these factors should contribute to less out-migration from the United States as the global population had a net positive supply of migration-age people and the United States had a shrinking net positive supply of migration age people compared to the baseline population. Indeed, the age-standardized net migration forecast for the United States was shifted towards higher net in-migration compared to the age-agnostic forecast.

The forecast MASI ratios for El Salvador and for South Africa were higher than the global MASI ratios and above the baseline period, indicating that the age-standardized migration forecast should be shifted towards more net out-migration compared to the age-agnostic forecast. The age-standardized net migration rate was indeed more negative than the age-agnostic migration rate for El Salvador. However, age-standardized and age-agnostic net migration forecasts were indistinguishable for South Africa given the relatively small share of population change attributable to migration.

The forecast MASI ratio for Saudi Arabia was higher than the global MASI ratio and above the baseline period, indicating that the age-standardized migration forecast should be shifted towards more net out-migration compared to the age-agnostic forecast if the forecasting methods were otherwise identical. However, the age-standardized approach to forecasting Gulf Cooperation Council (GCC) uses a different approach to GCC net migration forecasting that makes the age-standardized and age-agnostic comparisons less relevant in this case. Still, net migration forecasts generated from the age-standardized method were more similar to the observed rates. Since migration is the main contributor to population change in GCC countries, the small improvement in the age-standardized forecast led to a substantial improvement in the population forecast compared to the age-agnostic approach.

Multiple other forecast horizons were also evaluated. Predictions were generated one to four periods ahead of the last observed data. Out-of-sample forecasts use the last observed population age structure as the baseline, fit each model to data available prior to the first forecast period, and generate forecasts for each period through the 2015-2020 period. We generated one-period-ahead forecasts for periods starting in 2000, 2005, 2010, and 2015. Two-period-ahead forecasts were generated for periods starting in 2000, 2005, and 2010. Three-period-ahead forecasts were generated for periods starting in 2000 and 2005. The four-period-ahead forecast was generated for the period starting in 2000 only. We did not evaluate the five-period-ahead forecast as it is not possible to fit the mixed-effects model (1) with only one period of inflow and outflow data.

We evaluated the point forecasts in terms of the Mean Absolute Error (MAE), the Log Mean Absolute Error (LMAE), and the Mean Absolute Scaled Error (MASE). The

LMAE is defined as follows:

$$\begin{aligned}
 l(y) &= \text{sign}(y) [\log(|y| + c) - \log c] \quad \text{with } c > 0 \\
 \text{sign}(y) &= \begin{cases} 1 & y > 0 \\ 0 & y = 0 \\ -1 & y < 0 \end{cases} \\
 LMAE_t &= \frac{1}{200} \sum_{i=1}^{200} |l(f_{i,t}) - l(r_{i,t})|. \tag{14}
 \end{aligned}$$

We used $c = 1$. The LMAE formulation prevents large errors in a few forecasts from dominating the error metric.

The MASE, recommended by Hyndman & Koehler (2006), summarizes forecast performance in terms of the mean ratio of errors from a proposed method in the numerator and errors from a naïve method such as persistence forecast in the denominator. Error estimates in the denominator are estimated from mean errors of the naïve method using the in-sample data, e.g. mean net migration rate errors generated from the 1950-2000 data using the naïve method in the denominator compared to mean forecast error in the 2000-2020 data. Let $f_{i,t}$ denote the net migration rate forecast for country i and period starting in year t when the true net migration rate is $r_{i,t}$. The MASE of the forecast for T_k forecast periods and S_k in-sample periods starting in forecast period t_0 to $t_0 + 5$ and in-sample period s_0 to $s_0 + 5$ with a forecast horizon k periods ahead of the last observation is defined as

$$\text{MASE}_k = \frac{\frac{1}{200 \times T_k} \sum_{i=1}^{200} \sum_{\{t_0\}_k} |r_{i,t_0+5(k-1)} - f_{i,t_0+5(k-1)}|}{\frac{1}{200 \times S_k} \sum_{i=1}^{200} \sum_{\{s_0\}_k} |r_{i,s_0+5k} - r_{i,s_0}|}. \tag{15}$$

This formula leads to the ratio of average k -period ahead forecast errors for all possible horizons k in the in-sample and out-of-sample periods. For the $k = 1$ one-period-ahead forecasts, $\{t_0\}_1 = \{2000, 2005, 2010, 2015\}$, $T_1 = 4$, $\{s_0\}_1 = \{1950, 1955, \dots, 1990\}$, and $S_1 = 9$. For the $k = 4$ four-period-ahead forecast, $\{t_0\}_4 = \{2000\}$, $T_4 = 1$, $\{s_0\}_4 = \{1950, 1955, \dots, 1975\}$, and $S_4 = 6$.

Forecast calibration was evaluated in terms of 95% prediction interval coverage and average prediction half-interval width. If a model is well-calibrated, then 95% prediction intervals generated from the model should contain about 95% of the true net migration rate observations. Prediction intervals that contain less than 95% of the true values are too narrow, indicating that the model underestimates forecast variation. Prediction intervals that contain more than 95% of the true values are too wide, indicating that the model overestimates forecast variation. Prediction half-interval width is calculated as half the difference between the upper prediction interval quantile and lower prediction interval quantile. Accurate, well-calibrated models with smaller half-interval widths are preferred to models with the same accuracy and calibration estimates.

Table 2 summarizes out-of-sample predictive performance of the age-standardized, age-agnostic, and net rate persistence methods. Errors are calculated as the difference between the observed value and the median of 2,000 posterior predictive distribution draws. Rate persistence uses the last observed net rate in each country as the forecast. The best score for each method is shown in bold font.

The age-agnostic and net rate persistence models were fit using the bayesPop R package (Ševčíková & Raftery, 2016). The age-standardized model was fit using a custom

Table 2: Mean predictive performance of different methods for net migration rate (migrants per thousand period person years): mean absolute error (MAE), log mean absolute error (LMAE) with $c = 1$, mean absolute scaled error (MASE), 95% prediction interval coverage, and mean prediction interval half-width (HW).

	Method	MAE	LMAE	MASE	Cover	HW
5 Years	Persistence	4.02	0.68	1.42	—	—
	Agnostic	3.44	0.65	1.25	93	10.47
	Standardized	3.54	0.65	1.28	93	10.39
10 Years	Persistence	5.33	0.88	1.63	—	—
	Agnostic	3.86	0.76	1.16	91	11.63
	Standardized	3.93	0.77	1.17	90	11.44
15 Years	Persistence	5.16	1.00	1.44	—	—
	Agnostic	3.49	0.83	1.10	92	12.32
	Standardized	3.51	0.82	1.11	92	11.85
20 Years	Persistence	4.77	1.02	1.27	—	—
	Agnostic	2.91	0.82	1.00	94	12.54
	Standardized	2.86	0.79	0.98	94	12.04

implementation of the bayesPop R package. The age-standardized and the age-agnostic model accuracy were similar across all horizons, but age-standardized forecast accuracy overtakes age-agnostic forecast accuracy as the number of periods between the last observations and the forecast period increased for all metrics. The age-standardized model was better calibrated in terms of 95% prediction interval coverage for all horizons except the one-period-ahead forecast, but both models had slight under-coverage compared to the 95% nominal rate. The age-agnostic and age-standardized models outperformed the rate persistence model forecast in all horizons. Similarities between the agnostic and standardized model accuracy are expected over short forecast horizons since population age structure changes slowly.

5 Results

Figure 4 summarizes probabilistic population forecasts in four countries using the age-agnostic migration model from Azose et al. (2016), the population forecasts using the age-standardized migration model, and the projections from the 2019 World Population Prospects (WPP 2019) (United Nations, 2019). Columns of the figure correspond to the same country. Rows of the figure show forecasts through 2100 for the MASI ratio, the net migration rate, and total population.

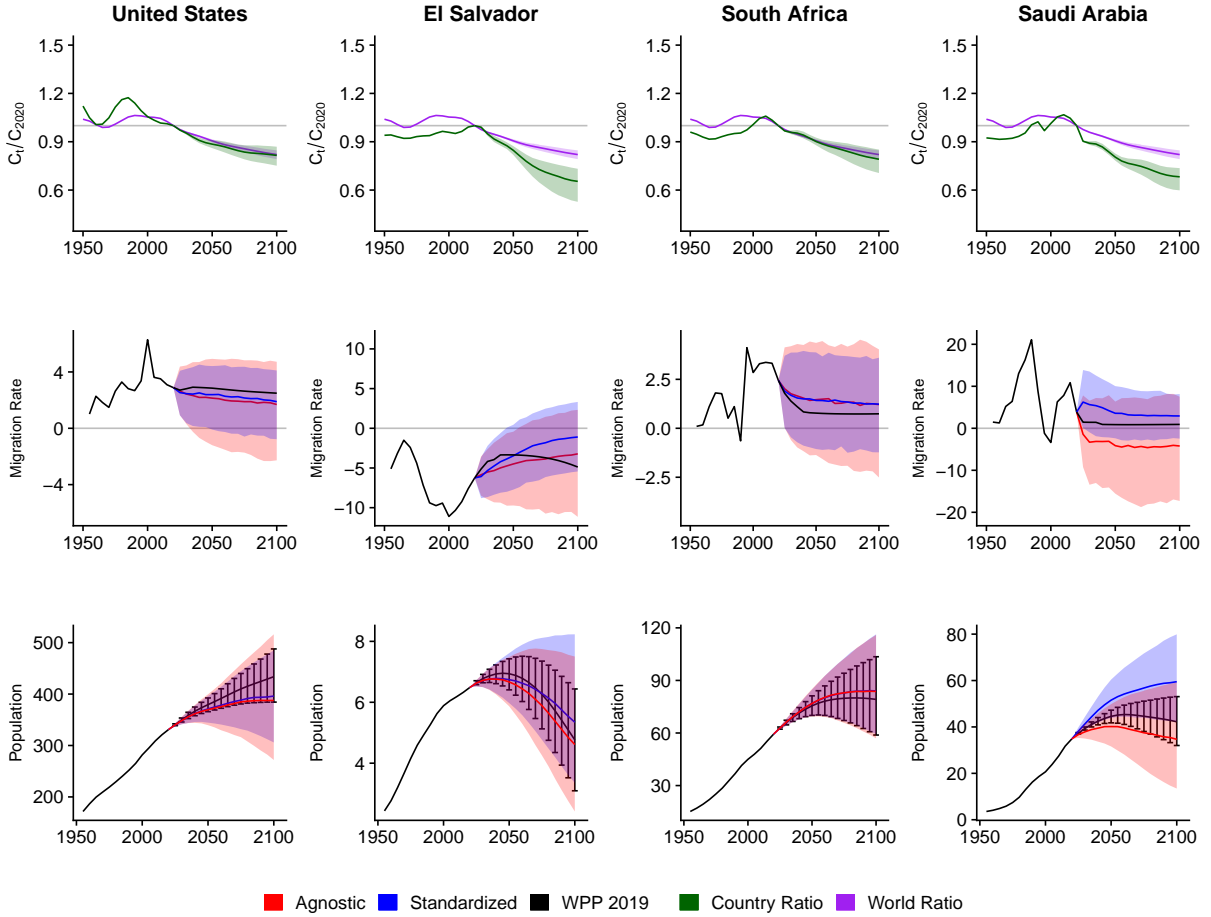


Figure 4: 2020 MASI ratios (top row), net migration rate as net annual migrants per thousand (middle row), and probabilistic forecast of population (in millions) age-standardized and age-agnostic (bottom row) for the United States, El Salvador, South Africa, and Saudi Arabia. Forecasts use probabilistic net migration (■=age-standardized and ■=age-agnostic), as well as probabilistic fertility, and mortality. The MASI ratio plots show the values for each country (■) and the world (■). Solid lines in each plot indicate the observed and median forecast. Shaded regions show the 80% prediction interval. Forecasts start in the 2020-2025 period.

The MASI ratios in the first row of Figure 4 summarize the differences in the population age structure from the 2020 baseline for each country (green) compared to the population age structure for the world (purple). Countries with a higher migration-age population than the 2020 population baseline rise above 1. Countries aging faster than the world population fall below the global index. Forecast population age structures in the United States and South Africa generally follow the global aging trend.

When the country-level MASI ratio is similar to the global one, then net migration forecasts from the age-standardized model and age-agnostic model should be more similar than in countries where the country-level and global MASI ratios diverge. The population age structures of El Salvador and Saudi Arabia are forecast to age much faster than the global average. In these cases, the age adjustment shifts the migration forecast towards higher net inflows, as we see for El Salvador and Saudi Arabia.

Median net migration forecasts from both probabilistic net migration models are similar in many countries, but long-term age-standardized net migration forecast intervals

tend to be narrower than age-agnostic forecast intervals. This is explained by the population age normalization step used in the age-standardized method. Age-standardized net migration rate variation attributable to variation in historic population age structure is removed before fitting the Azose & Raftery (2015) net migration model. Removing variation in past net migration estimates attributable to population age structure reduces the variance in the net migration model parameter estimates and hence the migration and population forecasts. Prediction intervals (80%) for both probabilistic net migration models include the United Nations' WPP 2019 projections through 2100 for all countries shown in Figure 4.

Median net migration forecasts from the age-agnostic and age-standardized methods are most similar in countries that have population age indices similar to the global population age index. The population age indices along with the median migration forecasts for the United States and South Africa in Figure 4 demonstrate this trend. Age-standardized migration forecasts in countries where the population age structure diverges from the global norm often leads to much different median migration forecasts compared to the age-agnostic migration model. For example, El Salvador's population is forecast to age much more rapidly from 2020 to 2100 compared to the global age structure. As a result, the median age-standardized net migration forecast is shifted towards lower net out-migration compared to the age-agnostic forecast. Since the age adjustment leads to less negative net migration, the age-standardized population forecast is higher than the forecast using the age-agnostic model. Furthermore, the age-standardized 80% prediction interval upper bound shows that there is less certainty that the population size will peak by 2100 compared to the age-agnostic model.

Figure 4 also shows that Saudi Arabia's population age structure is forecast to change about as fast as El Salvador's compared to the 2020 baseline population age structure. Saudi Arabia's net migration forecast is also shifted towards higher net in-migration, but this leads to a higher net positive migration forecast compared to the age-agnostic model. The age-standardized net positive migration forecast is better aligned to the historic net rate data in Saudi Arabia and the UN's WPP 2019 net migration forecast. Differences in Saudi Arabia's migration and population forecast using the age-standardized approach arise from both population age structure effects and adjustments to modeling unique features of migration in GCC countries. These adjustments lead to a substantially higher median population forecast and prediction interval. The UN WPP 2019 population forecast falls to the bottom of the age-standardized prediction interval compared to the upper middle of the interval using the age-agnostic model. See the supplemental index for detailed forecasts for all countries.

Figure 5 summarizes past and median forecast MASI ratios for the globe and several countries by global region. The MASI ratio provides a concise one-number summary of historic and forecast population age structure dynamics. While mean country and global age also summarize the degree of aging, the MASI is more informative in terms of assessing changes to the inherent force of migration attributable to the relevant populations at risk. The MASI explicitly weights age groups by a Rogers & Castro-like model migration age schedule. Taking the ratio of period MASI values puts the structural demographic force of migration potential within a country into the context of the reference population. The role of the MASI in removing the influence of population age structure is a more relevant measure of population age dynamics for migration than other measures that are less directly related to a population's structural migration potential, such as its average age.

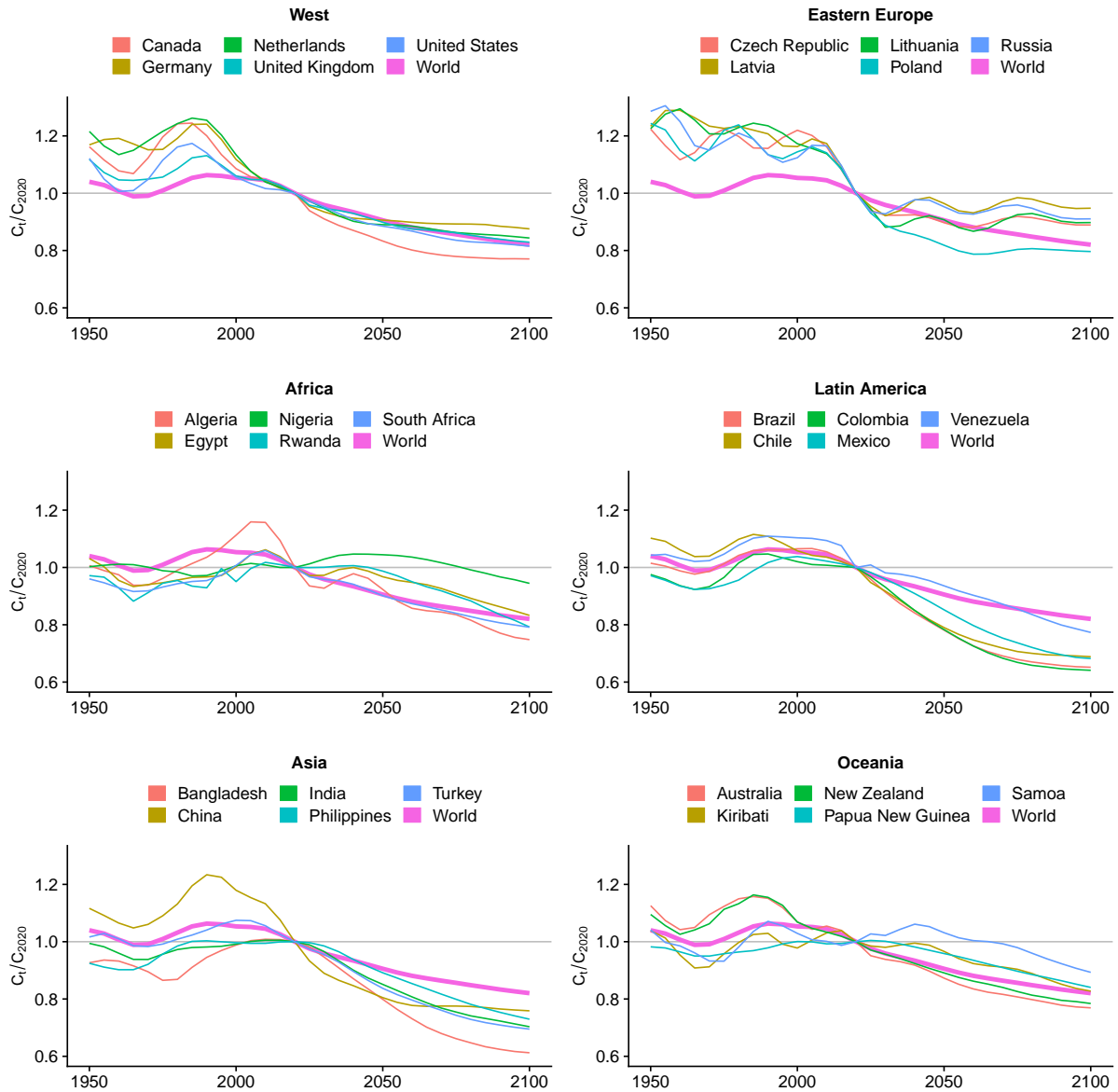


Figure 5: Historic and median country-level forecasts of MASI ratios for 2020 baseline by region compared to the world.

Figure 5 shows that the median population age structure forecasts in Western countries follows the global population aging trend. This indicates that the underlying force of out-migration in Western countries is forecast to align with the global average compared to the population age structure in 2020 and the median net migration forecasts from the age-standardized and age-agnostic methods will largely agree with one another. The underlying force of migration from Latin America by contrast falls sharply in coming decades compared to the 2020 baseline and the world overall, indicating that the force of out-migration will fall faster than the world on average and lead to higher net migration forecasts using the age-standardized method. The population age index forecast for some countries has yet to reach their peak, e.g. Rwanda in Africa and Samoa in Oceania. This implies that forecast out-migration from these countries is too small in the age-agnostic method.

Age-standardized migration forecasts led to less steep population declines in countries

facing the greatest demographic challenges. Figure 6 shows the age index, net migration, and population forecasts among large countries that anticipate some of the most drastic population contractions by 2100. The age-standardized net migration forecast leads to less severe population forecast declines than the age-agnostic forecast as there are fewer people of prime migration age in the population. The age index shows that the force of out-migration falls in these countries as they age compared to the rest of the world, shifting the net migration forecast towards higher in-migration compared to the age-agnostic forecast. Median age-standardized net migration forecasts in these countries are more similar to the UN's WPP 2019 migration and population forecasts than the age-agnostic forecasts.

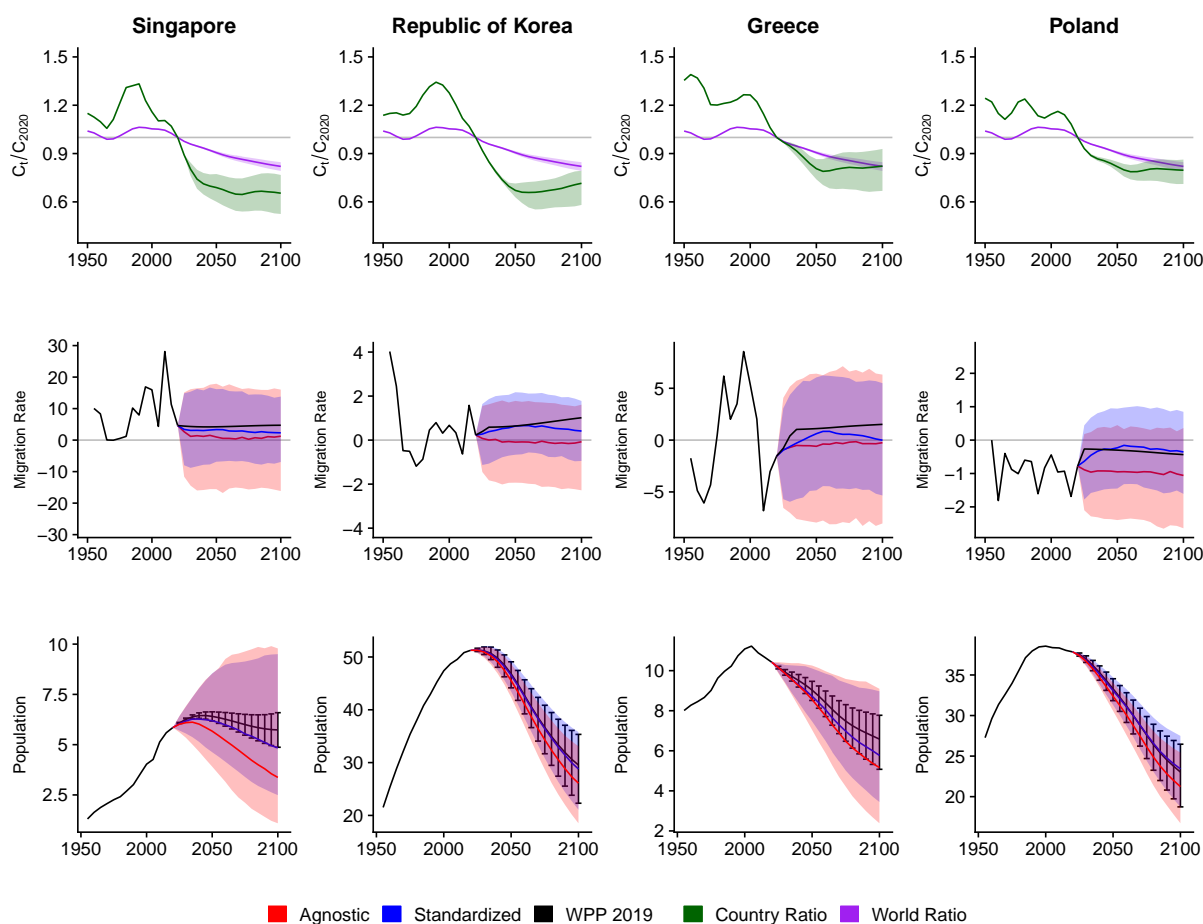


Figure 6: 2020 base-year MASI ratios (top row), age-standardized and age-agnostic net migration rate as net annual migrants per thousand (middle row), and probabilistic forecast of population (in millions) age-standardized and age-agnostic (bottom row) for Singapore, South Korea, Greece, Poland. Forecasts use probabilistic net migration (■=age-standardized and ■=age-agnostic), fertility, and mortality. Age-index ratio plots show the age structure ratios for each country (■) and world (■). Solid lines in each plot indicate the observed and median forecast. Shaded regions show the 80% prediction interval. Forecasts start in the 2020-2025 period.

Figure 7 shows the world and regional forecasts using the age-agnostic and age-standardized migration forecast models. World forecasts of population are indistinguishable, which makes sense as both methods use the same fertility and mortality models.

Global forecasts could have differed due to differences in fertility and mortality norms among migrants' destination countries, but these differences were not large enough to substantially alter the global population forecasts or overall uncertainty.

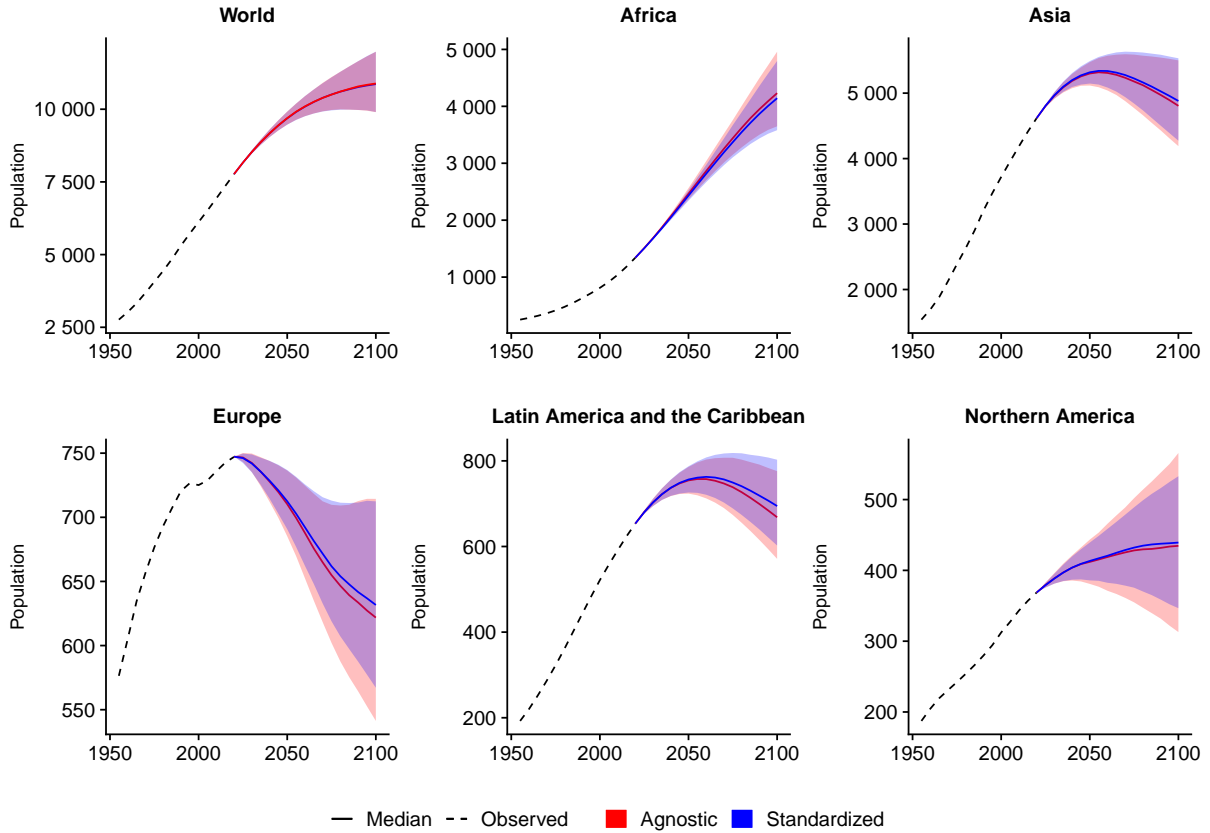


Figure 7: Probabilistic forecast of population (millions of people) by region. Forecasts use probabilistic net migration (■=age-standardized and ■=age-agnostic), fertility, and mortality. Solid lines indicate the median forecast. Dashed lines indicate the observed population. Shaded regions show the 80% prediction interval. Forecasts start in the 2020-2025 period.

Africa's population forecast by the end of the century is lower under the age-standardized model compared to the agnostic migration model. This makes sense because the force of migration associated with population age structure in many African countries is forecast to far exceed the global median for most of the remainder of the century. As a result, long-term forecasts that ignore population age structure for many countries in Africa are slightly overstated compared to the age standardized migration model. End-of-century median population forecasts for all other regions are higher using the age-standardized migration model.

The most pronounced differences are for Europe and North America. Age-standardized posterior prediction intervals for Europe and North America lie within the age-agnostic prediction intervals. The most extreme population declines in Europe and Latin America are less likely under the age-standardized model. Migration forecasts from the age-standardized model are lowered by aging populations in both regions. The most extreme population growth and decline trajectories in North America are less likely under the age-standardized model.

Table 3 details the differences in the population forecasts using the age-standardized and age-agnostic migration forecasting methods shown in Figure 7.

Table 3: Median population and net migration forecasts at the end of the century by United Nations Area and the world using age-standardized (S) and age-agnostic (A) migration forecasting in millions of people along with the net difference (S-A) and percent difference $100 \times \frac{S-A}{A}$ %.

UN Area	Measure	S	A	S - A	$100 \times \frac{S-A}{A}$ %
Africa	population	4142.6	4231.3	-88.7	-2.0
	net migration	-10.5	-6.3	-4.3	68.0
Asia	population	4880.3	4806.0	74.4	2.0
	net migration	0.1	-1.2	1.3	-109.0
Europe	population	631.6	621.8	9.8	2.0
	net migration	3.4	2.8	0.7	24.0
Latin America & the Caribbean	population	694.4	668.3	26.2	4.0
	net migration	0.7	-1.4	2.1	-153.0
Northern America	population	439.3	434.6	4.6	1.0
	net migration	4.4	3.9	0.5	12.0
Oceania	population	65.1	62.6	2.5	4.0
	net migration	0.4	0.2	0.2	132.0
World	population	10863.3	10884.4	-21.1	0.0

Figure 8 shows the population forecast differences at the end of this century for each country for three different forecasts. Each point denotes the departure of the median population forecast by 2100 using the age-agnostic or age-standardized migration model from the median WPP 2019 forecast. These ratios make it possible to evaluate differences in all three forecasts together. Points falling near the origin indicate approximate agreement between the age-agnostic, age-standardized, and WPP 2019 median population forecasts. Points on along $y = 0$ indicate agreement between median age-agnostic and WPP 2019 forecasts that differ from the age-standardized forecast. Points on $x = 0$ indicate agreement between the age-standardized forecast and the WPP 2019 forecast that differ from the age-agnostic forecast. Points on $y = x$ far from the origin denote agreement between the age-agnostic and age-standardized forecasts that depart from the WPP 2019 forecast. All other combinations are summarized by the plot regions bounded by the dashed lines and labeled I-VI on the plot.

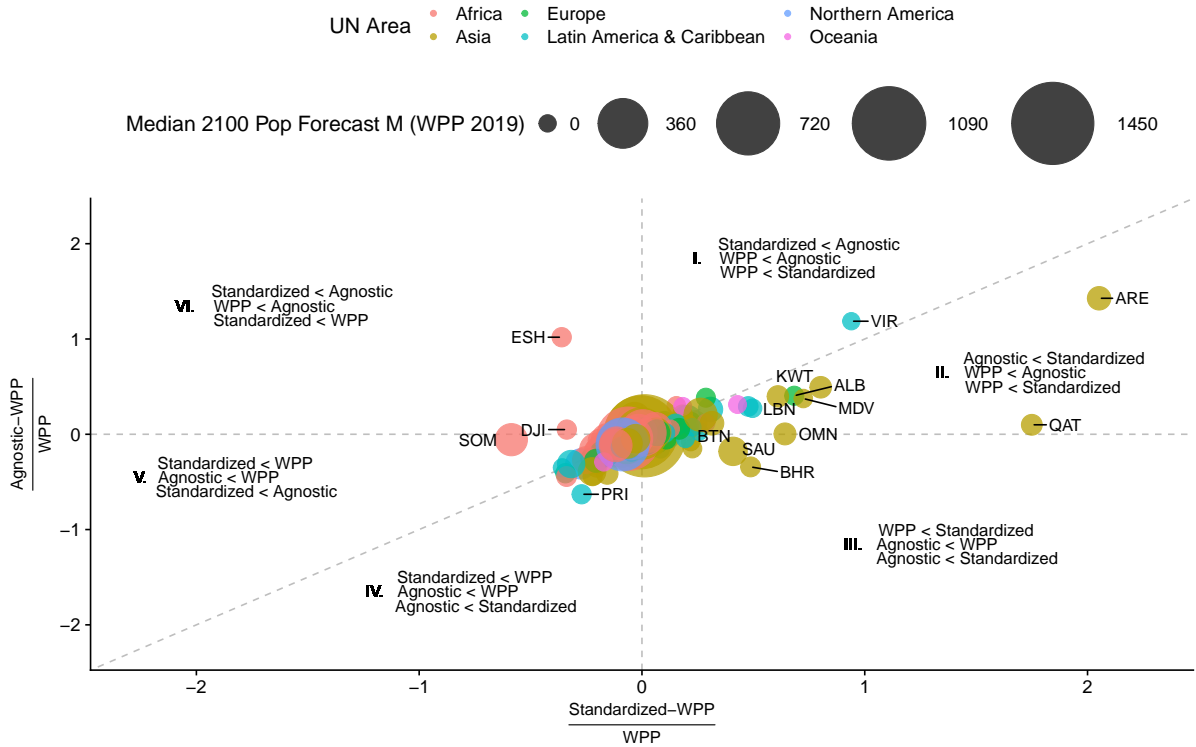


Figure 8: Three-way comparison of median 2100 population forecasts using age-standardized migration model, age-agnostic migration model, and median WPP 2019 forecast. Point color indicates UN Area, point diameter indicates WPP 2019 median population forecast size (millions), and regions I-VI show direction of forecast differences using the age-agnostic and age-standardized migration models.

Figure 8 shows that all three median population forecasts differ for Eastern Sahara (ESH). Both the age-agnostic and age-standardized methods lead to higher population forecasts for the United Arab Emirates (ARE) than WPP 2019, but the median age-standardized forecast is largest. The median age-standardized population forecast was highest among the three for all GCC countries. The age-standardized method generated fewer negative net migration trajectories over the forecast period; however, this outcome is consistent with the last three decades of sustained positive net migration that has been dominated by foreign workers responding to labor opportunities in rapidly expanding economies. Net migration rate forecasts using the age-standardized approach continue the net positive trend in GCC countries with expanding populations. While the age-standardized migration forecasts for GCC countries is higher than the age-agnostic approach, the population age structure in most GCC countries appears much more plausible and closer to the WPP 2019 forecast than the age-agnostic method.

The Supplementary Information includes forecasts for the 200 largest countries, associated quantiles, and additional information about the software used to generate these results.

6 Discussion

The association between migration and age is long established. However, we are unaware of any existing migration forecasting method that explicitly accounts for the influence of

overall population age structure, apart from that of Raftery & Ševčíková (2023), which relied on an unrealistic assumption. The potential support ratio (PSR), defined as the proportion of the working age population to the total population, has been used as a proxy for population age structure in other methods (K. Kim & Cohen, 2010). However this approach does not distinguish a population age distribution concentrated at ages 20-39 from one more heavily concentrated at ages 40-65, although the implications of these for migration are very different.

Our approach addresses multiple criticisms of using net migration as a unit of analysis. Our model-based approach to decompose the net flow rate into inflow and outflow rates alleviates the migration age schedule issues outlined in Rogers (1990). He also pointed out that relatively small net migration counts over a period can hide comparatively huge inflows and outflows of roughly equal magnitude. While net migration is the unit of analysis here, we use the historic data within a country to decompose net flow rate estimates into inflow and outflow rates. Dividing inflow and outflow counts by the age-standardized population size makes it possible to put flow rates from a diverse population of countries around the globe on the same scale for modeling and forecasting.

While the methods used in age-standardized net migration estimation and forecasting partly address long-standing criticisms of net migration rate analysis, a bilateral migration flow model among all countries as in Welch & Raftery (2022) eliminates theoretical challenges induced by the use of net migration rate as the unit of analysis. However, the computational complexity of migration flow forecasting and limited historic bilateral flow data reduce the viability of this alternative for longer-term forecasting. International bilateral migration flow forecasting among 200 countries involves estimating and forecasting 39,800 bilateral flows as opposed to 200 net flow rates. Furthermore, there are only six quinquennial periods of bilateral migration flow estimates available at present (Abel & Cohen, 2019) compared to thirteen periods for net migration (United Nations, 2019). Methods described in this article offer a more computationally tractable alternative to bilateral migration flow model fit to only half the historical net migration data.

Probabilistic forecasts offer a principled means to integrate uncertainty, but historic shocks to long-term trends arise without warning. Multiple such shocks occurred in the last ten years alone. The 2020 COVID-19 pandemic, Syria’s decade old civil war, Russia’s invasion in Ukraine, and the economic meltdown in Venezuela all upset long-term demographic norms—especially migration. New norms could take hold as a result of these and other crises, but the full effect of these historic events should be integrated into updated forecasts once the data become available. The age-standardized probabilistic migration forecasting method presented here includes well-defined mechanisms to account for changes to variation around long-term trends. When the full extent of recent crises emerges in the data, the forecasts should be revised with these data.

Using age-standardized net migration aims to eliminate the influence of population age structure on historic and forecast net migration rates, improving on existing probabilistic net migration forecasting methods. However, key drawbacks of the use of net migration are not completely addressed by our method. Shifts in net migration forecast due to changes in country population age structure are directly reflected in the forecast for the country of origin; however, using the population age structure of the globe to normalize inflow rates could be improved to more directly reflect the changes in population age structures of sending countries. For example, Mexico and Central American countries are currently the largest suppliers of immigrants to the United States. Calculating a country-specific inflow age ratio index to reflect that fact rather than a simple average of

the global population age distribution would more directly link changes in the population age structure of top sending countries on the age-standardized net migration rate. We chose to use the global average in our models because it is far simpler analytically and to account for the possibility that migration corridors that exist now could change in the future.

Our methods build on methodological advances made in the last decade (Azose & Raftery, 2015), address several known challenges with net migration as the unit of analysis (Rogers, 1990), and offer a more computationally tractable alternative to migration flow forecasting (Welch & Raftery, 2022). Our model-based approach to decomposing net migration rates into inflow and outflow rates offers an efficient alternative to more computationally challenging analyses involving direct modeling of bilateral migration flows. We propose a new method to account for unique differences in forecasting net flows in Gulf Cooperation Council countries that more accurately reflects migration dynamics in those countries in the future. Finally, we found the MASI ratio to be a concise one-number summary of the population age structure that measures the pace of aging expected to take place in the coming decades in the context of migration. Reducing the influence of population age structure on historic and forecast migration rates leads to more accurate long-term forecasts and matches or narrows the migration and population prediction intervals compared to a comparable age-agnostic method.

References

- Abel, G. J. (2013, January-June). Estimating Global Migration Flow Tables Using Place of Birth Data. *Demographic Research*, 28, 505-546.
- Abel, G. J., & Cohen, J. E. (2019, June). Bilateral International Migration Flow Estimates for 200 Countries. *Nature*, 6(82), 1-13.
- Azose, J. J., & Raftery, A. E. (2015). Bayesian Probabilistic Projection of International Migration. *Demography*, 52(5), 1627-1650.
- Azose, J. J., & Raftery, A. E. (2019). Estimation of Emigration, Return Migration, and Transit Migration Between All Pairs of Countries. *Proceedings of the National Academy of Sciences*, 116(1), 116-122.
- Azose, J. J., Ševčíková, H., & Raftery, A. E. (2016). Probabilistic Population Projections with Migration Uncertainty. *Proceedings of the National Academy of Sciences*, 113(23), 6460-6465.
- Bates, D., Mächler, M., Bolker, B., & Walker, S. (2015). Fitting Linear Mixed-Effects Models Using lme4. *Journal of Statistical Software*, 67(1), 1-48. doi: 10.18637/jss.v067.i01
- Bloom, D. E., & Zucker, L. M. (2023, June). *Aging is the Real Population Bomb* (Tech. Rep.). International Monetary Fund.
- Bongaarts, J. (2009). Human Population Growth and the Demographic Transition. *Philosophical Transactions of the Royal Society B: Biological Sciences*, 364(1532), 2985-2990.

- Coleman, D. (2008). The Demographic Effects of International Migration in Europe. *Oxford Review of Economic Policy*, 24(3), 452–476.
- Director of National Intelligence. (2021). *The Future of Migration* (Assessment No. NIC-2021-02486). United States Director of National Intelligence.
- Fertig, M., & Schmidt, C. M. (2005). Aggregate-level Migration Studies as a Tool for Forecasting Future Migration Streams. In *International Migration* (pp. 129–156). Routledge.
- Hyndman, R. J., & Booth, H. (2008). Stochastic Population Forecasts Using Functional Data Models for Mortality, Fertility and Migration. *International Journal of Forecasting*, 24(3), 323–342.
- Hyndman, R. J., & Koehler, A. B. (2006). Another Look at Measures of Forecast Accuracy. *International Journal of Forecasting*, 22(4), 679–688.
- Kim, C. J. (2019). *Aging Societies: Policies and Perspectives* (Tech. Rep.). Asian Development Bank Institute.
- Kim, K., & Cohen, J. E. (2010). Determinants of International Migration Flows to and from Industrialized Countries: A Panel Data Approach Beyond Gravity. *International Migration Review*, 44(4), 899–932.
- Kolk, M. (2019). Period and Cohort Measures of Internal Migration. *Population*, 74(3), 333–350.
- Kupiszewski, M. (2002). How Trustworthy Are Forecasts of International Migration Between Poland and the European Union? *Journal of Ethnic and Migration Studies*, 28(4), 627–645.
- Lee, R. (2011). The Outlook for Population Growth. *Science*, 333(6042), 569–573.
- Münz, R. (2013, September). *Demography and Migration: An Outlook for the 21st Century* (Policy Brief No. 4). Migration Policy Institute.
- Raftery, A. E., Alkema, L., & Gerland, P. (2014). Bayesian Population Projections for the United Nations. *Statistical Science*, 29(1), 58–68.
- Raftery, A. E., Li, N., Ševčíková, H., Gerland, P., & Heilig, G. K. (2012). Bayesian Probabilistic Population Projections for All Countries. *Proceedings of the National Academy of Sciences*, 109(35), 13915–13921.
- Raftery, A. E., & Ševčíková, H. (2023). Probabilistic Population Forecasting: Short to Very Long-Term. *International Journal of Forecasting*, 39(1), 73–97.
- RAND. (2005). *Population Implosion? Low Fertility and Policy Responses in the European Union* (Research Brief). Cambridge, UK: RAND Corporation.
- Raymer, J., Guan, Q., Shen, T., Hertog, S., & Gerland, P. (2023, December). *Modelling the Age and Sex Profiles of Net International Migration* (Technical Report No. UN DESA/POP/2023/TP/No. 7). New York: Department of Economic and Social Affairs, Population Division.

- Rogers, A. (1990). Requiem for the Net Migrant. *Geographical Analysis*, 22(4), 283–300.
- Rogers, A., & Castro, L. J. (1981). *Model Migration Schedules* (Research Report No. 81-30). Laxenburg, Austria: International Institute for Applied Systems Analysis.
- United Nations. (2019). *World Population Prospects 2019: Methodology of the United Nations Population Estimates and Projections* (Methodology Report No. ST/E-SA/SER.A/425). New York: Department of Economic and Social Affairs, Population Division.
- United Nations. (2022, July). *World Population Prospects 2022: Methodology of the United Nations Population Estimates and Projections* (Methodology Report No. UN DESA/POP/2022/DC/NO.6). New York: Department of Economic and Social Affairs, Population Division.
- Ševčíková, H., & Raftery, A. E. (2016). bayesPop: Probabilistic Population Projections. *Journal of Statistical Software*, 75(5), 1–29.
- Welch, N. G., & Raftery, A. E. (2022). Probabilistic Forecasts of International Bilateral Migration Flows. *Proceedings of the National Academy of Sciences*, 119(35), e2203822119.
- Wiśniowski, A., Smith, P. W., Bijak, J., Raymer, J., & Forster, J. J. (2015). Bayesian Population Forecasting: Extending the Lee-Carter Method. *Demography*, 52(3), 1035–1059.
- Woetzel, J., Madgavkar, A., Rifai, K., Mattern, F., Bughin, J., Manyika, J., . . . Hasyagar, A. (2016, December). *People on the Move: Global Migration's Impact and Opportunity* (Report). Mckinsey Global Institute.
- Yu, C. C., Ševčíková, H., Raftery, A. E., & Curran, S. R. (2023). Probabilistic County-Level Population Projections. *Demography*, 60(3), 915–937.

A Proof of Theorem 1

Proof. Starting from the definition of $\text{OMR}_{i,t}$,

$$\begin{aligned}
 \text{OMR}_{i,t} &= \frac{O_{i,t}}{\tilde{P}_{i,t,+,+}} && \text{(definition of OMR)} \\
 &= \sum_a \frac{O_{i,t,a}}{\tilde{P}_{i,t,a,+}} \times \frac{\tilde{P}_{i,t,a,+}}{\tilde{P}_{i,t,+,+}} && \text{(OMR disaggregated by age)} \\
 &= G_{i,t} \sum_a \frac{\text{OMR}_{i,t,a}}{G_{i,t}} \times \pi_{i,t,a} && \left(\text{Multiplication by } \frac{G_{i,t}}{G_{i,t}} \right).
 \end{aligned} \tag{16}$$

The same derivation applies to $\text{OMR}_{i,t}^*$, implying that

$$\text{OMR}_{i,t}^* = G_{i,t} \sum_a \frac{\text{OMR}_{i,t,a}}{G_{i,t}} \times \pi_{i,t,a}^*. \tag{17}$$

Rearranging $\text{OMR}_{i,t}$ in terms of $G_{i,t}$ and substituting the equation into (17) yields the desired result:

$$\text{OMR}_{i,t}^* = \text{OMR}_{i,t} \frac{\sum_a \text{OMR}_{i,t,a} \pi_{i,t,a}^*}{\sum_a \text{OMR}_{i,t,a} \pi_{i,t,a}}. \tag{18}$$

Multiplying (18) by $\frac{G_{i,t}}{G_{i,t}}$, assuming the same $R_a = \text{OMR}_{i,t,a}/G_{i,t}$ in both populations, and applying the definition of R_a , we obtain

$$\text{OMR}_{i,t}^* = \text{OMR}_{i,t} \frac{\sum_a R_a \pi_{i,t,a}^*}{\sum_a R_a \pi_{i,t,a}} = \text{OMR}_{i,t} \frac{C_{i,t}^*}{C_{i,t}}, \tag{19}$$

as desired. This concludes the proof. \square